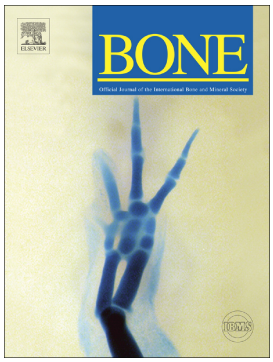

TNFα blockade mediates bone protection in antigen-induced arthritis by reducing osteoclast precursor supply

Stephanie Uster, Fernanda Matos Coelho, Daniel Aeberli, Jens V. Stein, Wilhelm Hofstetter, Britta Engelhardt, Michael Seitz

PII: S8756-3282(17)30386-1
DOI: doi:10.1016/j.bone.2017.10.020
Reference: BON 11460

To appear in: *Bone*

Received date: 6 July 2017
Revised date: 12 October 2017
Accepted date: 23 October 2017

Please cite this article as: Stephanie Uster, Fernanda Matos Coelho, Daniel Aeberli, Jens V. Stein, Wilhelm Hofstetter, Britta Engelhardt, Michael Seitz , TNFα blockade mediates bone protection in antigen-induced arthritis by reducing osteoclast precursor supply. The address for the corresponding author was captured as affiliation for all authors. Please check if appropriate. Bon(2017), doi:10.1016/j.bone.2017.10.020

TNFα blockade mediates bone protection in antigen - induced arthritis by reducing osteoclast precursor supply

Stephanie Uster[a,b,c], Fernanda Matos Coelho[b,2], Daniel Aeberli[a], Jens V Stein[b], Wilhelm Hofstetter[d1], Britta Engelhardt[b,1,**] bengel@tki.unibe.ch, Michael Seitz[a,1,*] michael.seitz@insel.ch

[a]Department of Rheumatology, Immunology & Allergology, University Hospital, Bern, Switzerland

[b]Theodor Kocher Institute, University of Bern, Bern, Switzerland

[c]Graduate School for Cellular and Biomedical Sciences, University of Bern, Bern, Switzerland

[d]Group of Bone Biology & Orthopedic Research, Department for Biomedical Research, University of Bern, Bern, Switzerland

[*]**Corresponding author at:** M. Seitz, Department of Rheumatology, Immunology & Allergology, University Hospital of Bern, CH-3010 Bern, Switzerland.

[**]Correspondence to: B. Engelhardt, Theodor Kocher Institute, University of Bern, CH-3010 Bern, Switzerland.

[1]these authors are co-principal investigators of this work

[2]present address: Institute for Infectious Diseases, University of Bern, Switzerland

Keywords

Arthritis, Blockade of TNFα, Bone Protection, Osteoclast Precursors

Abbreviations

AIA: antigen induced arthritis **TRAP:** tartrate resistant acidic phosphatase

OPC: osteoclast precursor cell **M-CSF:** macrophage colony stimulating factor

RANKL: receptor activator of NF-κB ligand **RA:** rheumatoid arthritis

mBSA: methylated bovine serum albumin **CFA:** complete Freund's adjuvant

IFA: incomplete Freund's adjuvant **BrdU:** bromodeoxyuridine **Lin:** Lineage

Abstract

Bone protective effects of TNFα inhibition in rheumathoid arthritis are thought to be mediated by inhibiting synovial osteoclast differentiation and activity. However, it has not been addressed, if TNFα inhibitors alter the pool of peripheral osteoclast precursor cells (OPCs). Here, we blocked TNFα function in C57BL/6 mice with antigen induced arthritis (AIA) using the soluble TNFα receptor etanercept. Synovial bone lesions and osteoclasts were markedly reduced upon Etanercept in the early chronic phase of AIA. Unexpectedly this was not associated with a reduced recruitment of circulating OPCs to the arthritic joint nor to reduced synovial inflammation. In contrast we found that OPC numbers in bone marrow and blood were significantly reduced. Overall our study suggests that arrest of osteoclast mediated bone lesions upon inhibition of TNFα is, at least initially, based on reduced OPC availability in the periphery, and not on OPC recruitment or local anti-inflammatory effects in the arthritic joint.

1. Introduction

Inflammation-induced bone lesions are a key feature in human rheumatoid arthritis (RA) and animal models of chronic arthritis [1, 2]. The differentiation of new bone resorbing osteoclasts in the arthritic joint critically depends on two essential factors: Macrophage colony stimulating factor (M-CSF) and receptor activator of NF-κB ligand (RANKL) [3, 4]. An additional requirement for synovial osteoclastogenesis is the availability of OPCs, which belong to the monocyte/macrophage lineage [5]. Monocytes are divided into two subsets, classical and non-classical monocytes, which in mice, can be distinguished by their Ly6C^{high}CX3CR1^{inter} and Ly6C^{low}CX3CR1^{high} marker expression, respectively [6]. After maturation in the bone marrow, classical and non-classical monocytes circulate in blood and become inflammatory macrophages upon recruitment to the site of inflammation. These infiltrating monocyte-derived macrophages are potent producers of pro-inflammatory cytokines and efficiently initiate immune responses [7, 8]. In contrast, tissue resident macrophages are considered to be more important for the maintenance and restoration of tissue integrity. Due to self-proliferation, they maintain themselves mostly independently of newly recruited hematopoietic cells [9, 10].

In RA, inflamed joints provide an optimal environment for the differentiation of bone resorbing osteoclasts [11]. On one side, M-CSF and RANKL expression is induced by the high level of pro-inflammatory cytokines [12, 13]; on the other side, continuous infiltration of circulating monocytes into the inflamed synovial compartment provides a cell pool that is

prone to differentiate into osteoclasts. The bone protective effect mediated by blockade of TNFα is well known and mostly explained by attenuation of inflammatory processes, favoring osteoclastogenesis within the arthritic joint [14, 15, 16]. However, there is emerging evidence, that anti-TNFα therapy affects osteoclastogenesis outside of the synovial compartment. TNFα has been associated with alterations in the pool of peripheral OPCs [17]. Furthermore, patients that were treated with TNFα inhibitors showed a bone protective effect that was not dependent on the inflammation in the arthritic joint [18]. Although myeloid markers were previously used to characterize OPC populations, the precise distinction between different monocyte subsets was often not completely taken into consideration [17, 19].

In the present study, we used heterozygous CX3CR1-GFP knock-in mice and attributed an osteoclastogenic potential to the classical Ly6C^{high}CX3CR1^{inter} monocyte subset. We demonstrate that in an AIA mouse model TNFα inhibition reduced availability of these OPCs in bone marrow and blood without affecting their recruitment to the still highly inflamed joint.

2. Materials and methods

2.1. Animals and experimental arthritis model

C57BL/6J mice were obtained from Janvier (Genest Saint Isle, France). CX3CR1-GFP knock-in mice (Cx3cr1^{tm1Litt}) were kindly provided by Israel F. Charo (Gladstone Institute of Cardiovascular Research, University of California, San Francisco, USA). TNFR1/2 $^{-/-}$ (B6.129S-Tnfrsf1a^{tm1Imx}Tnfrsf1b^{tm1Imx}/J) mice were obtained from Jackson Laboratory (Bar Habor, Maine, USA). All mouse lines were backcrossed to C57BL/6J background for at least eight generations. Mice were housed in individually ventilated cages under specific pathogen-free conditions with water and food *ad libitum*. Animal procedures were performed in accordance with the Swiss legislation on the protection of animals and were approved under the application number BE 18/12 and BE 55/15 by the veterinary office of the Canton of Bern.

AIA was induced in 6-8 weeks old female mice using a previously described protocol [20]. Briefly, mice were immunized by subcutaneous injection of 100µg methylated bovine serum albumin (mBSA) (Sigma) in complete Freund's adjuvant (CFA) on day -21 and in incomplete Freund's adjuvant (IFA) (Santa Cruz Biotechnology, Inc) on day -14. CFA was additionally supplemented with 4mg/ml heat-killed Mycobacterium tuberculosis strain H37RA (Becton, Dickinson and Company). In parallel to each immunization, 200ng of *Bordetella pertussis* toxin (List biological laboratories, inc., Campbell, CA, USA) was administrated by an intraperitoneal injection. Arthritis was induced by injecting 100µg of mBSA in 20µl

physiologic saline into the knee joint, whereas injection of saline was used as sham control for the contralateral knee. 10mg/kg of etanercept (Enbrel®, Pfizer) or human polyclonal IgG (BioXCell) was subcutaneously injected every other day after arthritis induction.

2.2. Adoptive transfer of monocytes

Monocytes were isolated from bone marrow and enriched by using CD115 MicroBead kit (MACS, miltenyibiotec). Cells were labelled with CSFE (Thermofisher, 1:1000 dilution) at 37°C for 20 minutes. 5 x 10^6 cells were injected via the femoral artery into AIA WT mice on day 14. After 30–60 minutes, periarticular tissue was harvested and recruitment of $CD45^{high}CD11b^{+}CSFE^{+}$ monocytes was quantified by flow cytometry.

2.3. Flow cytometry of bone marrow, blood and periarticular cells

200µg bromodeoxyuridine (BrdU) was intravenously injected and mice were euthanized after 30 minutes. Using flow cytometry, local cell proliferation was analyzed by BrdU incorporation in cells from femora and periarticular tissues. Cell surface staining was performed for 1h at 4°C. For additional intracellular BrdU staining, cells were incubated in Cytofix/Cytoperm Buffer (BDBioscience). Cells were kept in 10% DMSO at -80°C. After thawing, cells were refixed and treated with 300µg/ml DNAse for 1h at 37°C and stained for BrdU. Total blood count was determined with a scil VetABC™ Hematology Analyzer (Scil animal care company, Viernheim, Germany). Total cell count of bone marrow and periarticular tissue was determined by using PKH26 reference microbeads (Sigma). Samples were measured with the LSR II (BDBioscience) and data were analyzed with the FlowJo software.

2.4. Monocyte sorting and in vitro osteoclast cultures

Bone marrow cells were harvested from CX3CR1-GFP knock-in mice and stained with anti-CD117 antibody. Non-classical monocytes were defined as CX3CR1-GFP^{high}CD117^{-} and classical monocytes as CX3CR1-GFP^{inter}CD117^{-}. For sorting from blood, non-classical and classical monocytes were defined by their CX3CR1-GFP^{high} and CX3CR1-GFP^{inter} expression, respectively, and blood from mice with on-going arthritis from AIA day 3 was used. Sorting was performed by using ARIA flow cytometry (BDBioscience). 30`000 cells were distributed in a 48-well plate and cultured in complete α-MEM medium supplemented with 30ng/ml M-CSF and 50ng/ml RANKL at 37°C. After 5 days for bone marrow and after 14 days for blood cultures, cells were fixed, stained for TRAP (Sigma) and the number of multinucleated TRAP^{+} osteoclasts/well was determined.

2.5. Histology, immunohistochemistry and microCT

Mice were perfused with 4% PFA and knee joints were harvested. After overnight post-fixation, knees were decalcified in 15% EDTA and paraffin embedded. One section of each knee was sagittally cut through the center of the joint and stained with H&E and for TRAP, respectively. Synovial inflammation on H&E stained knee sections were scored as followed: perivascular leukocyte infiltration (0-5), synovial leukocyte infiltration (0-5), synovial hyperplasia (0-5). Bone parameters on H&E knee sections were scored by bone erosion severity on meniscus (0-4) and tibial joint surface (0-4). Synovial osteoclasts on TRAP stained knee sections was scored by TRAP^{+} osteoclasts located on the meniscus (0-3) and tibial bone surface (0-3). For immunohistochemistry, knee sections were incubated for 1h with primary rat and secondary rabbit anti-rat antibody. A system-HRP labeled polymer anti-rabbit (Envision Dako) was added for 30min on paraffin sections. Sections were washed and incubated in the substrate solution with AEC tablets. F4/80 and Gr-1 staining was scored by intensity (0-5) in the complete synovial compartment and the bone surface area.

Undecalcified tibia from CX3CR1-GFP knock-in mice were sectioned by using the CryoJane Tape-Transfer System (Leica) according to Jiang et al [21]. MicroCT analysis was done 14 days after arthritis onset in IgG (n=4) and etanercept (n=4) treated mice.

2.6. Serum Chemokines in non-arthritic and arthritic mice with and without etanercept treatment.

Circulating chemokines from non-arthritic as well as arthritic mice with and without anti-TNF treatment with etanercept were measured in serum 14 days after onset of arthritis. For this purpose a membrane – based antibody array/sandwich immunoassay from R&D Systems (Bio – Techne AG, Zug, Switzerland) was used to detect 25 chemokines in mouse serum samples.

2.7. Antibodies for flow cytometry

All rat anti-mouse monoclonal antibodies used for flow cytometry were purchased from BioLegend: anti-Ly6G (18A), anti-CD45 (30-F11), anti-CD115 (AFS98), anti-CD117 (2B8), anti-CD11b (M1/70), anti-Ly6C (HK1.4), anti-BrdU (Bu20a), anti-NK1.1 (PK136), anti-B220 (RA3-6B2), anti-CD19 (6D5), anti-SiglecF (E50-2440), anti-CD90.2 (30-H12), IgG1, κ (RTK2071), IgG2a, κ (RTK2758), IgG2b, κ (RTK4530). Negative controls were done with unspecific isotype antibodies.

2.8. Antibodies for histology

Rat anti-mouse F4/80 (clone CI:A3-1, produced in house). Rat anti-mouse Gr-1 (NIMP-R14, Abcam). Rat IgG2b, κ (RTK4530, BioLegend)

2.9. Statistical analyses

Statistical analysis was performed using GraphPad Prism 6.0 software (Graphpad software, La Jolla, CA, USA). Data were compared by Mann-Whitney test. Asterisks indicate significant differences (*P<0.05, **P<0.01 and***P<0.001, ****P<0.0001).

3. Results

3.1. Antigen - induced arthritis leads to recruitment of monocytic osteoclast precursors and osteoclastogenesis in inflamed knees

In order to investigate if TNFα affects synovial osteoclastogenesis on the level of osteoclast precursors, we chose AIA as an animal model in which synovial inflammation and bone destruction is associated with continuous recruitment of circulating leukocytes/osteoclast precursors. The antigen injection into the knee cavity of mice that were previously two times immunized with adjuvants-antigen solutions, led to a marked increase in synovial cellularity as determined by histology of the knee joint already at day 3 post knee-injection. In the early chronic phase of AIA, 14 days after knee-injection, synovial histopathology was additionally associated with pannus formation and alterations in joint architecture (Fig. 1A). Analysis by flow cytometry of periarticular tissue revealed two different $CD45^+$ leukocyte populations in knee joints of sham-treated and AIA mice. While non-inflamed knee joints of sham-treated mice only harbored tissue resident $CD45^{inter}$ cells, periarticular tissues of arthritic knees showed infiltration of $CD45^{high}$ leukocytes (Fig. 1B, left). The total number of these infiltrating $CD45^{high}$ leukocytes increased in arthritic knees from AIA day 3 to 14 (Fig. 1B, right). As a next step, we investigated whether infiltration of $CD45^{high}$ leukocytes was associated with the appearance of new bone resorbing osteoclasts. In contrast to the osteoclast-free synovium of uninflamed sham knees and arthritic knees from day 3, $TRAP^+$

osteoclasts were found adjacent to tibial bone lesions in the early chronic phase on day 14 of AIA (Fig. 1C). We hypothesized that the presence of synovial monocytes/macrophages was prerequisite for the observed osteoclastogenesis in the arthritic joint on day 14. We defined synovial monocyte/macrophages as $CD45^{high}CD11b^{+}$ $Lineage^{neg}$ cells since it has been shown that the recruitment of monocytic osteoclast precursors from the blood to the knee joint rapidly induces expression of complex marker sets related to tissue macrophage differentiation [8]. By using the gating strategy shown in the FACS plots in Fig. 1D (left), the amount of synovial monocytes/macrophages was quantified in the acute and early chronic phase of AIA. Indeed, increased infiltration of these osteoclast precursor cells correlated with the appearance of synovial osteoclasts and structural damage in the knee joint on day 14 of AIA (Fig. 1 D, right).

3.2. Classical monocytes rather than non-classical monocytes exhibit osteoclastogenic properties

We observed in the early chronic phase of AIA, 14 days after arthritis induction, osteoclast-mediated bone resorption, which was associated with infiltration of monocytes/ macrophages. This suggested that recruitment of monocytic osteoclast precursors substantially contributed to these new synovial bone lesions. To investigate which monocyte subsets hold the potential to differentiate into osteoclasts, we took advantage of CX3CR1-GFP knock-in mice, in which CX3CR1 promoter activity drives expression of GFP and thus allows distinction of classical and non-classical monocytes. We confirmed that classical CX3CR1-GFP^{inter} and non-classical CX3CR1-GFP^{high} bone marrow monocytes expressed monocytic markers such as CD11b and CD115 (Supplementary Fig. 1A). Bone marrow cells were isolated and classical CX3CR1-GFP^{inter} and non-classical CX3CR1-GFP^{high} monocytes that were negative for the bone marrow precursor marker c-kit/CD117, were sorted by flow

cytometry (Fig. 2A). After 4-6 days of culture under pro-osteoclastogenic conditions in the presence of M-CSF and RANKL, $TRAP^+$ osteoclasts were counted. While mixed bone marrow cells and classical CX3CR1-GFP^{inter} monocytes gave rise to osteoclasts, non-classical CX3CR1-GFP^{high} monocytes failed to develop into osteoclasts (Fig. 2B and C). Bone marrow contains in addition to monocytes also macrophages and dendritic cells, which may as well express CX3CR1. In contrast, CX3CR1-GFP expression in monocytes of the blood was over 90% associated with monocytic markers (Supplementary Fig. 1B). We therefore used blood from AIA mice for isolating and sorting monocytes to avoid any contaminations by differentiated macrophages. Consistent with bone marrow cells, only classical, but not non-classical blood monocytes differentiated into osteoclasts *in vitro* (Fig. 2D). The *in vitro* condition allowing monocytes to differentiate into osteoclasts may not fully mimic their respective osteoclastogenic potential *in vivo*. Hence, tibiae from the *sham* control side of CX3CR1-GFP knock-in mice were used for cryosections and the osteoclastogenic characteristics of the two monocyte subsets were analyzed by co-localization of endogenous CX3CR1-GFP^+ and stained $TRAP^+$ cells *in situ*. GFP^+ bone marrow cells could clearly be divided into a CX3CR1-GFP^{inter} and CX3CR1-GFP^{high} population. Mature $TRAP^+$ osteoclasts on the bone surface did not express CX3CR1-GFP. However, in the bone marrow cavity nearby the bone surface, CX3CR1-GFP^{inter} cells were found to be co-localized with TRAP staining, indicating that late $TRAP^+$ osteoclast precursor cells show a classical monocyte phenotype (Fig. 2E).

3.3. Anti-TNFα therapy reduces bone lesions and the number of synovial osteoclasts

To elucidate the precise role of TNFα on bone resorbing osteoclasts and their precursor cells, we confirmed as a proof of concept that TNFα contributed to AIA pathogenesis. Arthritis was induced in TNFR1/2 $^{-/-}$ C57BL/6 mice, lacking both receptors for TNFα. Indeed, TNFR1/2 $^{-/-}$ C57BL/6 mice showed significantly ameliorated arthritis in terms of synovial inflammation

and reduced numbers of TRAP$^+$ osteoclasts in the knee joint on day 14 of AIA (Supplementary Fig. 2A and B). To have a clinically more relevant experimental setup, AIA was induced in WT C57BL/6 mice, which were from then on treated every second day with 10mg/kg TNFα antagonist, the soluble TNFα receptor etanercept. Inhibition of TNFα had a bone protective effect, which was reflected by fewer pathological bone lesions (Fig. 3A) and a reduced number of synovial TRAP$^+$ osteoclasts in the knee joint on day 14 of AIA (Fig. 3B). However, despite the reduced synovial osteoclastogenesis, etanercept treated mice still showed highly inflamed knee joints that were infiltrated with leukocytes (Fig. 3C).

3.4. TNFα blockade reduces the number of synovial Gr-1$^+$ monocytes but not their recruitment to the arthritic joint

In order to examine if the previously observed bone protective effect in etanercept treated animals was based on changes in the OPC population, myeloid marker expression in different tissues was analyzed by immunohistochemistry and flow cytometry at acute and chronic timepoints of AIA. In the acute phase on day 3, knee immunohistochemistry of control and etanercept treated mice did not reveal any changes in terms of the presence of synovial F4/80$^+$ and Gr-1$^+$ myeloid cells. In line with this, the amount of infiltrating CD45^{high} leukocytes in sham and arthritic knees was not different between both treatment groups as shown by flow cytometry (Supplementary Fig. 3A and B). Furthermore, neither bone marrow nor blood showed any difference in leukocyte and monocyte numbers between control and etanercept treated mice on AIA day 3. Only the number of neutrophils was slightly reduced in the blood of anti-TNFα treated animals on day 3 (Supplementary Fig. 4 A and B).

In contrast to day 3, etanercept treatment resulted in clear cellular changes in the synovial compartment in the early chronic phase on day 14 of AIA. Although anti-TNFα therapy did not result in any significant difference in the availability of F4/80$^+$ macrophages (Fig. 4A,

upper panel), etanercept treatment markedly reduced the number of Gr-1^{+} cells, a mixed population of neutrophils and Ly6C^{high} monocytes/macrophages in the inflamed joint (Fig. 4A, lower panel). Since we previously observed that classical Ly6C^{high} monocytes efficiently differentiated into osteoclasts *in vitro*, it is noteworthy, that these Ly6C^{high}Ly6G^{+} cells were often found in the synovial lining nearby the bone lesions on the tibial joint surface of control treated mice. Interestingly, arthritic knees of control and etanercept treated animals did not show any difference in the number of infiltrating CD45^{high} leukocytes (Fig. 4B).

It has been reported that tissue resident cells often show increased proliferation rates upon inflammation and thereby substantially contribute with infiltrating cells to the increased amount of synovial cells [9]. We therefore examined if alterations in local cell proliferation contributed to the different knee cellularity observed on day 14 of AIA. A short-term incorporation of BrdU into dividing synovial cells was done. Only few tissue resident CD45^{inter}CD11b^{+} macrophages showed some proliferation, which was, however, not different between the control and etanercept treatment group. In contrast, infiltrating CD45^{high} leukocytes did not show any proliferative properties in control and Etanercept treated mice and their number was therefore attributable to their recruitment from blood (Fig. 4C). To address the question if the lower number of synovial Gr-1^{+} cells upon anti-TNFα therapy was based on reduced recruitment of osteoclast precursors into the joint, an adoptive transfer of monocytes was performed on day 14 after arthritis onset. Bone marrow cells were harvested and enriched for CD115^{+} monocytes, then labeled with CSFE and adoptively transferred into the femoral artery of arthritic mice. After 30 minutes, periarticular tissue from inflamed knees was harvested and analyzed for infiltrating CD45^{high}CD11b^{+}CSFE^{+} cells by flow cytometry (Fig. 4D, left). The recruitment of adoptively transferred CSFE^{+} monocytes into the arthritic knee was not different between etanercept and control treated animals

supporting the notion that etanercept does not directly influence monocyte recruitment into the inflamed joint (Fig. 4D, right).

3.5. *Anti-TNFα therapy leads to fewer circulating and proliferating monocytic osteoclast precursors in blood and bone marrow, respectively*

Since neither synovial inflammation nor monocyte recruitment from blood to synovial tissue was affected by anti-TNFα therapy, we were wondering if changes in peripheral OPC populations led to fewer osteoclasts in the inflamed joint of etanercept treated mice. We therefore analyzed the cellular composition of bone marrow and blood by flow cytometry. Indeed, in bone marrow, etanercept treated mice showed despite unchanged numbers of total $CD45^+$ leukocytes, fewer $Ly6G^+$ neutrophils and more importantly, fewer proliferating $BrdU^+$ monocyte precursors (Fig. 5A and B). This was accompanied by a dramatic reduction of the numbers of circulating monocytes. Etanercept treated mice harbored fewer circulating classical $Ly6C^{high}$ monocytes and $Ly6G^+$ neutrophils, while the total number of circulating $CD45^+$ leukocytes remained unchanged (Fig. 5C). These data nicely correlated with the decreased number of $Gr\text{-}1^+$ myeloid cells and osteoclasts found in synovial tissue of etanercept treated animals.

3.6. *Anti-TNFα therapy does not regulate circulating chemokine levels in arthritic and non-arthritic mice*

14 days after onset of arthritis we checked for serum levels of 25 different chemokines (CCL11/eotaxin, CCL12/MCP-5, CCL2/JE/MCP-1, CCL21/6 Ckine, CCL22/MDC, CCL27/CTACK, CCL28, CCL3/CCL4 (MIP-1alpha/MIP-1beta), CCL5/RANTES, CCL6/C10, CCL8/MCP-2, CCL9/MIP-1 gamma, Chemerin, Complement Component C%/C5a, CX3CL1/Fractalkine, CXCL1/KC, CXCL10/IP-10/CRG-2, CXCL11/I-TAC, CXCL12/SDF-1, CXCL13/BLC/BCA-1, CXCL16, CXCL2/MIP-2, CXCL9/MIG, IL-16, LIX).

Serum levels of mice in the following experimental settings were checked: non-arthritic controls (n=4), non-arthritic but etanercept-treated (n=4), arthritic (n=4), arthritic and etanercept-treated (n=4). However, we found no statistically significant differences of circulating chemokine levels. The data are shown in a supplementary figure 5.

4. Discussion

In the present study we asked to which degree anti-TNFα therapy reduces osteoclast mediated bone resorption by affecting osteoclast precursor cells. We examined if availability of OPCs in bone marrow, blood and synovia and their recruitment to the arthritic knee was reduced upon blockade of TNFα. As a first step, we aimed to characterize the mouse osteoclast precursor populations, which belong to the monocyte/macrophage lineage. OPCs were previously defined by using general monocytic markers, however, the distinction between the two known classical and non-classical monocyte subpopulations, Ly6C^{high}CX3CR^{inter} respectively, was rarely applied [17, 19]. Interestingly, there is increasing evidence that, not only in terms of osteoclastogenic potential, these monocyte subsets play key roles for different aspects in RA pathogenesis [8, 22, 23]. Sorting CX3CR1^{inter} and CX3CR1^{high} monocytes by flow cytometry from bone marrow and blood showed that the osteoclastogenic potential was restricted to classical monocytes, which is also supported by findings in humans [24]. We also found a difference in the maturation and the number of osteoclasts between the culture from bone marrow and blood. We can only speculate that one probable explanation might be the higher number of macrophages and of Ly6high cells in bone marrow compared to blood that are able to proliferate [25,26]. Moreover, bone marrow contains the more complex composition of proliferating progenitor cells and matured macrophages [27]. This is also reflected by the non-homogeneous cell population in bone marrow compared to the homogeneous cell population in blood as shown in

supplementary Figure 1. Classical monocytes are known for their efficient recruitment to the site of infection [6]. Thus we hypothesized that infiltration of circulating monocytes into the arthritic knee is key for newly formed bone lesions by giving rise to bone resorbing osteoclasts in the arthritic joint. In accordance with this, it has been shown in parabiosis experiments that circulating GFP^+ monocytes from CX3CR1-GFP knock-in mice differentiated into mature GFP^+ osteoclasts in bone tissue of WT mice [28]. However, we also detected over the course of AIA low numbers of proliferating tissue resident $CD45^{inter}$ macrophages in inflamed and non-inflamed knees. We cannot fully exclude that these tissue resident macrophages might also give rise to osteoclasts in our model. However, tissue resident macrophages are known for their specific tissue-related tasks and their mature phenotype, which argues against their plasticity as OPCs [9, 10]. Having defined the monocytic OPC population, we were wondering if the observed bone protective effect upon anti-TNFα therapy can be attributed to reduced recruitment of circulating monocytes to the inflamed knee. TNFα and other inflammatory cytokines are key effector molecules regulating leukocyte migration as they efficiently upregulate endothelial cell adhesion molecules at the site of inflammation [29]. Surprisingly, the recruitment of adoptively transferred monocytes into the inflamed knee was not different between control and etanercept treated mice, which might be explained by the still strong on-going inflammation in the knee at this timepoint of arthritis in our model. In accordance with this, the number of infiltrated $CD45^{high}$ leukocytes and the synovial inflammation in knees of etancercept treated mice were not reduced on day 14 post knee-injection.

Similar to RA patients, who showed bone protection irrespective of the clinical response (pain and joint swelling), to anti-TNF therapy [18, 30], we found lower numbers of osteoclasts and bone lesions in still inflamed joints. In contrast, by MicroCT analyses we saw

no differences in cortical and trabecular volumes and densities in knees from AIA control and etanerept treated mice. One explanation could be that the time point of 14 days after induction of AIA was too early for morphometric bone analysis to detect significant differences in AIA with and without anti-TNF treatment. However, our data demonstrate that TNFα inhibition affects synovial osteoclastogenesis beyond the synovial compartment in the arthritic joint. Indeed, we showed that TNFα inhibition critically reduced the pool of proliferating bone marrow monocytic OPCs. This observations is in line with other studies, which reported that absence of TNFα reduced the number of immature myeloid cells in the bone marrow [31]. Even more impressive was the marked reduction of circulating classical monocytes in the blood of etanercept treated mice on day 14 after arthritis onset. One possible explanation for their lower number in blood would be cell death. However, infliximab treated RA patients did not show any signs of apoptosis in peripheral blood monocytes [32]. More likely, TNFα seemed to diminish the pool of circulating OPCs by first affecting monocytic precursor cells in bone marrow leading to a subsequently reduced number of monocytes released into blood. This assumption is finally in line with our observations that treatment with etanercept markedly reduced the number of Gr-1^{+} cells, a mixed myeloid population of neutrophils and $Ly6C^{high}$ monocytes/macrophages in the inflamed joint and that classical $Ly6C^{high}$ monocytes efficiently differentiated into osteoclasts *in vitro* and were often found in the synovial lining nearby the bone lesions on the tibial joint surface of control treated mice. Although we cannot exclude that etanercept additionally reduced osteoclast-inducing pro-inflammatory cytokine expression in the joint , we could clearly demonstrate a concordant decrease of OPCs of myeloid origin in bone marrow, peripheral blood and in the inflamed synovial tissue upon anti-TNFα treatment of arthritic mice. In light of our observations that adoptively transferred monocytes home equally well

to the inflamed joints of etanercept and sham treated mice our data strongly suggest that etanercept reduced monocyte supply from bone marrow rather than monocyte migration into the joint.

In accordance with this, TNFα was shown to reduce expression of CXCL12 in the bone marrow, which led to OPC release into the blood [33]. Moreover, our results also nicely correspond to the rapid decline in the number of circulating classical monocytes, the reduced expression of CXC chemokine receptor 4, C-C chemokine receptor type 2 and circulating stromal cell-derived factor-1 observed in patients with RA responding to anti-TNFα treatment with infliximab [34]. However, this could not be observed in our experimental AIA setting. 14 days after arthritis onset treatment with etanercept did not change the levels of circulating chemokines. Either this time period of ongoing arthritis was still too short to find any significant regulation of chemokines that could explain the downregulation of the number of circulating classical monocytes and neutrophils or the reduced peripheral cell numbers did merely reflect the failing supply from bone marrow. The missed chemokine regulation upon etanercept treatment also makes it less probable that altered proinflammatory cytokine profile was responsible for reduced numbers of circulating classical monocytes and neutrophils, although we cannot exclude that anti-TNFα treatment might have affected immune cells in lymph nodes such as Th17 cells that are associated with neutrophil accumulation and chemokine receptor expression.

Overall, the current study demonstrates that the bone protective effect mediated by blocking TNFα does not seem to mainly depend on direct inhibition of the synovial inflammation in the arthritic joint but may rather rely on limiting OPC supply from the bone marrow, thus limiting the number of monocytes circulating in the blood and able to migrate into the arthritic joint.

5. Limitations

Our study had several limitations. First, our experimental approach did not allow to directly correlate OPC numbers in different compartments with the synovial osteoclastogenesis. Second, the number of experiments showing the reduction of proliferating bone marrow monocyte precursors was relatively low to draw definite conclusions. Third, we did not correlate the number of osteoclastogenic cells in the synovial compartment with alterations of synovial inflammatory cytokine milieu upon anti-TNFα treatment that could have influenced directed cellular influx although synovial inflammation was still ongoing despite reduced synovial osteoclastogenesis and reduced bone destruction. Fourth, we did not discern if AIA treatment with etanercept did affect immune cells in local lymph nodes such as Th17 which might be associated with neutrophil accumulation and chemokine receptor expression.

6. Conclusion

Although being largely descriptive, our findings indicate that anti-TNFα treatment with etanercept had a bone protective effect in AIA of the mouse. This effect was not merely a consequence of downregulation of the inflammatory synovial response but conincided with the simultaneous reduction of numbers of osteoclast precursor cells in bone marrow, blood and synovial tissue and therefore suggested a reduced supply from the bone marrow. Our data point to the necessity of subsequent studies using cell tracking approaches to follow up the fate of bone marrow and blood OPCs over the entire course of arthritis [35].

Conflict of interest

The authors declare no financial or commercial conflict of interest.

Acknowledgements

We acknowledge Dr. Israel F Charo (Gladstone Institute of Cardiovascular Research, University of California, San Francisco, USA) and Dr. Richard Ransohoff (Biogen Idec, Cambridge, MA, USA) for graciously providing the CX3CR1-GFP knock-in mice. We thank Silvia Dolder, Irena Klima, Mark Siegrist, Heidi Tardent , Regina Reissmann , Dr. Juliana Barreto de Albuquerque and Antoinette Wetterwald for expert technical assistance and the animal caretakers Katrin Bisseger, Irina Geiger and Svetolzar Tsonev for excellent care of the animals. We also thank Matthias Hedinger from the Department of Biochemistry for letting us use his equipment for analysing the serum chemokine blots. Last but not least we thank Dr. Urban Deutsch for expert managing of our mouse colonies according to the 3R rules.

Funding

This study was funded by the Swiss National Science Foundation grant 310030_138459 to MS, BE, JVS, DA and WH, by the scientific fund of the Department of Rheumatology, Immunology & Allergology, University Hospital of Bern, Switzerland, and by the SNSF and Swissuniversities funded ProDoc „Cell Migration“ to BE and JVS. SU was enrolled in the Graduate School for Biomedical and Cellular Sciences of the University of Bern.

All procedures were performed in accordance with the Swiss legislation on the protection of animals and were approved under the application number BE 18/12 and BE 55/15 by the veterinary office of the Canton of Bern.

Authors Contributions

SU performed and analyzed all experiments and wrote the manuscript. FMC contributed to AIA experiments and analysis and contributed to writing the manuscript. DA, JVS, WH, BE and MS designed and supervised the study and were involved in drafting the article or

revising it critically for important intellectual contents; MS and BE have full access to all of the data in the study and take responsibility for the integrity of the data and the accuracy of the data analysis. All authors declare their consent for publication of this manuscript

References

[1] McInnes, I. B., and G. Schett. The Pathogenesis of Rheumatoid Arthritis. N Engl J Med. 365 (23) (2011) 2205-2219.

[2] Kollias, G., P. Papadaki, F. Apparailly, M. J. Vervoordeldonk, R. Holmdahl, V. Baumans, C. Desaintes, et al. Animal Models for Arthritis: Innovative Tools for Prevention and Treatment. Ann Rheum Dis. 70 (8) (2011) 1357-1362.

[3] Suda T, Nakamura I, Jimi E, Takahashi N. Regulation of osteoclast function. J Bone Miner Res. 12 (6) (1997) 869-879.

[4] Karsenty G. The genetic transformation of bone biology. Genes Dev. 13 (23) (1999) 3037-3051.

[5] Tondravi, M. M., et al. (1997). Osteopetrosis in mice lacking haematopoietic transcription factor PU.1. Nature. 386 (6620) (1997) 81-84.

[6] Geissmann, F., S. Jung, and D. R. Littman. Blood Monocytes Consist of Two Principal Subsets with Distinct Migratory Properties. Immunity. 19 (1) (2003) 71-82.

[7] Ginhoux, F., and S. Jung. Monocytes and Macrophages: Developmental Pathways and Tissue Homeostasis. Nat Rev Immunol. 14 (6) (2014) 392-404.

[8] Misharin, Alexander V, Carla M Cuda, Rana Saber, Jason D Turner, Angelica K Gierut, G. Kenneth Haines, Sergejs Berdnikovs, et al. Nonclassical Ly6c− Monocytes Drive the Development of Inflammatory Arthritis in Mice. Cell Reports. 9 (2) (2014) 591-604.

[9] Davies, L. C., et al. A quantifiable proliferative burst of tissue macrophages restores homeostatic macrophage populations after acute inflammation. Eur J Immunol . 41 (8) (2011) 2155-2164.

[10] Hashimoto, D., A. Chow, C. Noizat, P. Teo, M. B. Beasley, M. Leboeuf, C. D. Becker, et al. Tissue-Resident Macrophages Self-Maintain Locally Throughout Adult Life with Minimal Contribution from Circulating Monocytes. Immunity. 38 (4) (2013) 792-804.

[11] Redlich, K., and J. S. Smolen. Inflammatory Bone Loss: Pathogenesis and Therapeutic Intervention. Nat Rev Drug Discov. 11 (3) (2012) 234-250.

[12] Yao, Z., P. Li, Q. Zhang, E. M. Schwarz, P. Keng, A. Arbini, B. F. Boyce, and L. Xing. Tumor Necrosis Factor-Alpha Increases Circulating Osteoclast Precursor Numbers by Promoting Their Proliferation and Differentiation in the Bone Marrow through up-Regulation of C-Fms Expression. J Biol Chem. 281 (17) (2006) 11846-11855.

[13] Lee CK, Lee EY, Chung SM, Mun SH, Yoo B, Moon HB. Effects of disease – modifying antirheumatic drugs and anti-inflammatory cytokines on human osteoclastogenesis through interaction with receptor activator of nuclear factor kappa B, osteoprotegerin, and receptor activator of nuclear factor kappa B ligand. Arthritis Rheum. 50 (12) (2004) 3831 – 3843.

[14] Redlich, K., B. Gortz, S. Hayer, J. Zwerina, N. Doerr, P. Kostenuik, H. Bergmeister, et al. Repair of Local Bone Erosions and Reversal of Systemic Bone Loss Upon Therapy with Anti-Tumor Necrosis Factor in Combination with Osteoprotegerin or Parathyroid Hormone in Tumor Necrosis Factor-Mediated Arthritis. Am J Pathol. 164 (2) (2004) 543-55.

[15] Marotte H, Miossec P. Prevention of bone mineral density loss in patients with rheumatoid arthritis treated with anti-TNFalpha therapy. Biologics. 2 (4) (2008) 663-669.

[16] Ritchlin CT, Haas-Smith SA, Li P, Hicks DG, Schwarz EM. Mechanisms of TNFα – and RANKL – mediated osteoclastogenesis and bone resorption in psoriatic arthritis. J Clin Invest. 111 (6) (2003) 821-831.

[17] Li, P., E. M. Schwarz, R. J. O'Keefe, L. Ma, B. F. Boyce, and L. Xing. Rank Signaling Is Not Required for Tnfalpha-Mediated Increase in Cd11(Hi) Osteoclast Precursors but Is Essential for Mature Osteoclast Formation in Tnfalpha-Mediated Inflammatory Arthritis. J Bone Miner Res. 19 (2) (2004) 207-213.

[18] Smolen JS, Han C, Bala M, Maini RN, Kalden JR, van der Heijde D, Breedveld FC, Furst DE, Lipsky PE, ATTRACT Study Group. Evidence of radiographic benefit of treatment with infliximab plus methotrexate in rheumatoid arthritis patients who had no clinical improvement: a detailed subanalysis of data from the anti-tumor necrosis factor trial in rheumatoid arthritis with concomitant therapy study. Arthritis Rheum. 52 (4) (2005) 1020-1030.

[19] Ishii, M., J. G. Egen, F. Klauschen, M. Meier-Schellersheim, Y. Saeki, J. Vacher, R. L. Proia, and R. N. Germain. Sphingosine-1-Phosphate Mobilizes Osteoclast Precursors and Regulates Bone Homeostasis. Nature. 458 (7237) (2009) 524-528.

[20] Brackertz, D, Mitchell GF, Mackay IR. Antigen-induced arthritis in mice. I. Induction of arthritis in various strains of mice. Arthritis Rheum. 20 (3) (1977) 841-850.

[21] Jiang X, Kalajzic Z, Maye P, Braut A, Bellizzi J, Mina M, Rowe DW. Histological analysis of GFP expression in murine bone. Journal Histochem Cytochem. 53 (5) (2005) 593-602.

[22] Bruhl, H., J. Cihak, J. Plachy, L. Kunz-Schughart, M. Niedermeier, A. Denzel, M. Rodriguez Gomez, et al. Targeting of Gr-1+,Ccr2+ Monocytes in Collagen-Induced Arthritis. Arthritis Rheum. 56 (9) (2007) 2975-2985.

[23] Nanki, T., Y. Urasaki, T. Imai, M. Nishimura, K. Muramoto, T. Kubota, and N. Miyasaka. Inhibition of Fractalkine Ameliorates Murine Collagen-Induced Arthritis. J Immunol. 173 (11) (2004) 7010-7016.

[24] Komano, Y., T. Nanki, K. Hayashida, K. Taniguchi, and N. Miyasaka. Identification of a Human Peripheral Blood Monocyte Subset That Differentiates into Osteoclasts. Arthritis Res Ther. 8 (2006) R152.

[25] Engel, DR, Maurer J, Tittel AP, Weiheit C, Cavlar T, Schmak B, Limmer A, van Rooijen N, Trautwein C, Tacke F, Kurts C. CCR2 mediates homeostatic and inflammatory release of Gr1 (high) monocytes from the bone marrow, but is dispensable for bladder infiltration in bacterial urinary tract infection. J Immunol. 181 (8) (2008) 5579-5586.

[26] Rosas M, Thomas B, Stacey M, Gordon S, Taylor PR. The myeloid 7/4-antigen defines recently generated inflammatory macrophages and is synonymous with Ly-6B. J Leukoc Biol. 88 (1) (2010) 169-180.

[27] Hettinger J, Richards DM, Hansson J, Barra MM, Joschko AC, Krijgsveld J, and M. Feuerer. Origin of monocytes and macrophages in a committed progenitor. Nat Immunol. 14 (2013) 821-830.

[28] Kotani, M., J. Kikuta, F. Klauschen, T. Chino, Y. Kobayashi, H. Yasuda, K. Tamai, et al. Systemic Circulation and Bone Recruitment of Osteoclast Precursors Tracked by Using Fluorescent Imaging Techniques. J Immunol. 190 (2) (2013) 605-612.

[29] Tak PP, Taylor PC, Breedveld FC, Smeets TJ, Daha MR, Kluin PM, Meinders AE, Maini RN. Decrease in cellularity and expression of adhesion molecules by anti-tumor necrosis

factor α monoclonal antibody treatment in patients with rheumatoid arthritis. Arthritis Rheum. 39 (7) (1996) 1077-1081.

[30] Hoff M, Kvien TK, Kälvesten J, Elden A, Kavanaugh A, Haugeberg G. Adalimumab reduces hand bone loss in rheumatoid arthritis independent of clinical response: subanalysis of the PREMIER study. BMC Musculoskelet Disord. 12 (2011) 54.

[31] Sade-Feldman, M., J. Kanterman, E. Ish-Shalom, M. Elnekave, E. Horwitz, and M. Baniyash. Tumor Necrosis Factor-Alpha Blocks Differentiation and Enhances Suppressive Activity of Immature Myeloid Cells During Chronic Inflammation. Immunity. 38 (3) (2013) 541-554.

[32] Wijbrandts, C. A., P. H. Remans, P. L. Klarenbeek, D. Wouters, M. A. van den Bergh Weerman, T. J. Smeets, M. J. Vervoordeldonk, D. Baeten, and P. P. Tak. Analysis of Apoptosis in Peripheral Blood and Synovial Tissue Very Early after Initiation of Infliximab Treatment in Rheumatoid Arthritis Patients. Arthritis Rheum. 58 (10) (2008) 3330-3339.

[33] Zhang, Q., R. Guo, E. M. Schwarz, B. F. Boyce, and L. Xing. Tnf Inhibits Production of Stromal Cell-Derived Factor 1 by Bone Stromal Cells and Increases Osteoclast Precursor Mobilization from Bone Marrow to Peripheral Blood. Arthritis Res Ther. 10 (2008) R37.

[34] Aeberli, D., R. Kamgang, D. Balani, W. Hofstetter, P.M. Villiger, and M. Seitz. Regulation of Peripheral Classical and Non-Classical Monocytes on Infliximab Treatment in Patients with Rheumatoid Arthritis and Ankylosing Spondylitis. RMD Open. 2 (1) (2016) e000079.

[35] Shand, F. H., S. Ueha, M. Otsuji, S. S. Koid, S. Shichino, T. Tsukui, M. Kosugi-Kanaya, et al. Tracking of Intertissue Migration Reveals the Origins of Tumor-Infiltrating Monocytes. Proc Natl Acad Sci U S A. 111 (21) (2014) 7771-7776.

Figure Legends

Fig. 1: Infiltration of leukocytes and monocytic osteoclast precursors into the arthritic knee is associated with the appearance of synovial osteoclasts. A) H&E staining shows synovial cellularity of non-inflamed sham knee (left) and arthritic knees from AIA day 3 (center) and day 14 (right). → (synovial infiltrates), x (pannus). Scale bar = 200µm. Graph shows histological scoring of synovial inflammation of sham group (n=3 mice) and of AIA day 3 and day 14 groups (n= 5 mice each). B) Leukocyte cellularity of periarticular tissue was analyzed over arthritis course by flow cytometry. Contour plots show CD45 vs. SSC with percentage of tissue resident $CD45^{inter}$ myeloid cells (black gates) and infiltrating $CD45^{high}$ leukocytes (colored gates), respectively, in uninflamed sham knees (left) and arthritic knees from AIA day 3 (center) and day 14 (right). Numbers of infiltrating leukocytes are shown from a single experiment (n=4 mice) representative of two experiments performed. C) TRAP staining on paraffin sections shows osteoclasts in sham knee (left) and arthritic knees from AIA day 3 (center) and day 14 (right). → (synovial osteoclasts) Scale bar = 200µm. Graph shows histological scoring in knees of sham group (n=2 mice) and of AIA day 3 and day 14 groups (n= 5 mice each). D) Cellularity of periarticular tissues was analyzed by flow cytometry and the number of infiltrating monocytes/macrophages was determined. Contour plots illustrate

gating strategy for $CD45^{high}CD11b^{+}Lin^{neg}$ monocytes/macrophages. Colored gates in SSC vs. CD45 and CD11b vs. Lin plot highlight leukocyte populations that were gated on. Lineage markers = CD19, B220, NK1.1, Ly6G, Thy1, SiglecF. Numbers of infiltrating macrophages are from a single experiment (n=4 mice) representative of two experiments performed.

Fig. 2: Classical monocytes show osteoclastogenic properties. A) Classical and non-classical monocytes were sorted by flow cytometry using bone marrow from heterozygous CX3CR1-GFP knock-in mice. CX3CR1-GFP vs. CD117 contour plot depicts gates that were used to sort classical CX3CR1-GFP^{inter} and non-classical CX3CR1-GFP^{high} monocytes, respectively. B) Representative pictures of control bone marrow cells (left), sorted classical (center) and non-classical (right) monocytes after 5 days of osteoclastogenic culture. C) Number of multinucleated $TRAP^{+}$ osteoclasts/well was counted after 4, 5 and 6 days of cultures and shown as mean + SEM of three samples/replicates from one experiment representative of three experiments performed. D) Classical and non-classical monocytes were sorted from blood and cultured for 13 days. Number of multinucleated $TRAP^{+}$ osteoclasts/well was counted after 13 days of culture and are shown as mean + SEM of three wells/replicates from one experiment. E) Cryosection of undecalcified tibia from one heterozygous CX3CR1-GFP knock-in mice show CX3CR1-GFP expressing cells (left) and TRAP stained cells (right) which was analyzed for co-localization (arrows). Blue lines depict bone surface. Scale bar = 100µm *(data shown from a non-arthritic sham knee)*.

Fig. 3: Blockade of TNFα by etanercept reduces bone lesions and osteoclasts in the synovial compartment of AIA mice. A) H&E staining shows bone parameters of sham knee (left) and arthritic knees from control (center) and etanercept (right) treated group from AIA day 14. X

(pathological bone lesions). Scale bar = 400µm. Graphs shows scoring of pathological bone lesions pooled from three independent experiments (n=12 mice). B) TRAP staining shows synovial osteoclasts of uninflamed sham knee (left) and arthritic knees from control (center) and etanercept (right) group. Scale bar = 200µm. Graph depicts scoring for synovial osteoclasts pooled from two independent experiments (n=8 mice). C) H&E staining shows synovial inflammation and data shown are pooled from three independent experiments (n=12 mice). → (synovial infiltrates). Scale bar = 200µm.

Fig. 4: Anti-TNFα therapy reduces number of synovial Gr-1^{+} cells without affecting overall monocyte recruitment to the arthritic knee in the early chronic phase of arthritis. A) F4/80 (top) and Gr-1 (bottom) staining shows distribution of synovial macrophages and classical monocytes/neutrophils in sham knee (left) and arthritic knees of the control (center) and the Etanercept (right) group, respectively. Scale bar = 200µm. Histological knee scores represent individual observations pooled from two experiments (n=8 mice). B) Cellularity of periarticular tissue of sham knees and arthritic knees from AIA day 14 was analyzed by flow cytometry and the number of infiltrating CD45^{high} leukocytes all groups was determined. Numbers of infiltrating leukocytes are shown from one experiment (n=4 mice) representative of two experiments performed. C) Local cell proliferation in the synovial compartment was analyzed by short-term incorporation of BrdU. The graphs depict number of BrdU^{+} leukocytes within tissue-resident CD45^{inter} (left) and infiltrating CD45^{high} (right) leukocytes. Numbers of BrdU^{+} leukocytes are shown from one experiment (n=4 mice) representative of two experiments performed. D) Adoptively transferred CSFE labelled monocytes were quantified in periarticular tissues of mice from AIA day 14. Colored gates in the contour plots depict representative percentages of CD11b^{+}CSFE^{+} cells within CD45^{high}

leukocytes of control and etanercept treated mice, respectively. The number of recruited myeloid cells are pooled from two independent experiments (n=4 mice).

Fig. 5: Anti-TNFα therapy with Etanercept reduces the number of circulating classical monocytes and neutrophils and number of neutrophils and proliferating monocyte precursors in bone marrow. A) Local cell proliferation in the bone marrow compartment was analyzed by short-term incorporation of BrdU. Contour plots show representative percentages of $BrdU^+$ cells within $CD115^+Ly6C^{high}$ monocytes of control and etanercept group, respectively. Number of BrdU incorporated cells within $CD115^+Ly6C^{high}$ monocytes was determined in one experiment (n=4 mice). B) $CD45^+$ leukocyte, $Ly6G^+$ neutrophil and classical $Ly6C^{high}$ monocyte number in the bone marrow was determined and data shown are from one experiment (n=4 mice). C) Graphs represent number of circulating $CD45^+$ leukocytes, $Ly6G^+$ neutrophils and classical $Ly6C^{high}$ in the blood of control and etanercept treated mice on AIA day 14. Data shown are pooled from three independent experiments (n=12 mice).

Supplementary files

Supplementary Figure Legends

Supplementary Fig. 1: Characterization of classical and non-classical monocytes in CX3CR1-GFP knock-in mice. A) Contour plot shows CX3CR1-GFP vs. Ly6C and gates that were used for characterization of classical Ly6C^{high}CX3CR1-GFP^{inter} monocytes and non-classical Ly6C^{low}CX3CR1-GFP^{high} monocytes in bone marrow of CX3CR1-GFP knock-in mice. Contour plots in the colored boxes show percentages of CD115 and CD11b expressing cells within the previously gated classical and non-classical monocyte populations, respectively. B) Contour plot shows CX3CR1-GFP vs. Ly6C and depicted gates were used for characterization of classical Ly6C^{high}CX3CR1-GFP^{inter} monocytes and non-classical Ly6C^{low}CX3CR1-GFP^{high} monocytes in the blood of CX3CR1-GFP knock-in mice. Contour plots in the colored boxes show percentages of CD115 and CD11b expressing cells within the previously gated classical and non-classical monocyte populations, respectively.

Supplementary Fig. 2: TNFα is a critical player in the AIA pathogenesis. A) H&E staining shows synovial cellularity of non-inflamed sham knee (left) and arthritic knees from WT (center) and TNFR1/2 $^{-/-}$ (right) mice. Scale bar = 200µm. Knees were stained and scored for synovial inflammation. Histological scores are shown from one experiment with 3 mice B) TRAP staining on paraffin sections shows synovial distribution of osteoclasts in sham knee (left) and arthritic knees from WT (center) and TNFR1/2 $^{-/-}$ (right) mice. Scale bar = 200µm.

Knees were stained and scored for amount of synovial osteoclasts. Histological scores are shown are from one experiment with 3 mice.

Supplementary Fig. 3: TNFα inhibition has no effect on knee synovial cellularity in the acute phase of arthritis. A) F4/80 (top) and Gr-1 (bottom) staining show distribution of synovial macrophage and classical monocyte/neutrophil in uninflamed sham knee (left) and arthritic knees of control (center) and etanercept (right) treated group, respectively. Scale bar = 200µm. Knees were scored for synovial distribution of stained cells and graphs show individual observations pooled from two independent experiments (n=8 mice). B) Contour plots show CD45 vs. SSC with percentage of tissue resident $CD45^{inter}$ and infiltrating $CD45^{high}$ leukocyte population, respectively. Sham knees and knees from AIA day 14 were analyzed by flow cytometry and number of infiltrating $CD45^{high}$ leukocytes in the periarticular tissue of both treatment groups was determined. Numbers of infiltrating leukocytes are shown from one experiment (n=4 mice) representative of two experiments performed.

Supplementary Fig. 4: TNFα inhibition has no effect on bone marrow and blood cellularity in the acute phase of arthritis. A) Graphs show numbers of $CD45^{+}$ leukocytes, $Ly6G^{+}$ neutrophils and classical $Ly6C^{high}$ monocytes in the bone marrow. Data were obtained from one experiment (n=4 mice) representative of two experiments performed. B) Numbers of circulating $CD45^{+}$ leukocytes, $Ly6G^{+}$ neutrophils and classical $Ly6C^{high}$ and non-classical $Ly6C^{low}$ monocytes were determined in the blood. Data shown are pooled from four independent experiments (n=16 mice).

Supplementary Fig 5: TNFα inhibition has no effect on circulating chemokine levels. Graphs show the relative protein expression of various chemokines compared to gp130 14 days

after the induction of AIA in the serum of untreated control mice (n=4), non-arthritic mice treated with etanercept (n=4), untreated arthritic mice (n=4) and of arthritic mice treated with etanercept (n=4).

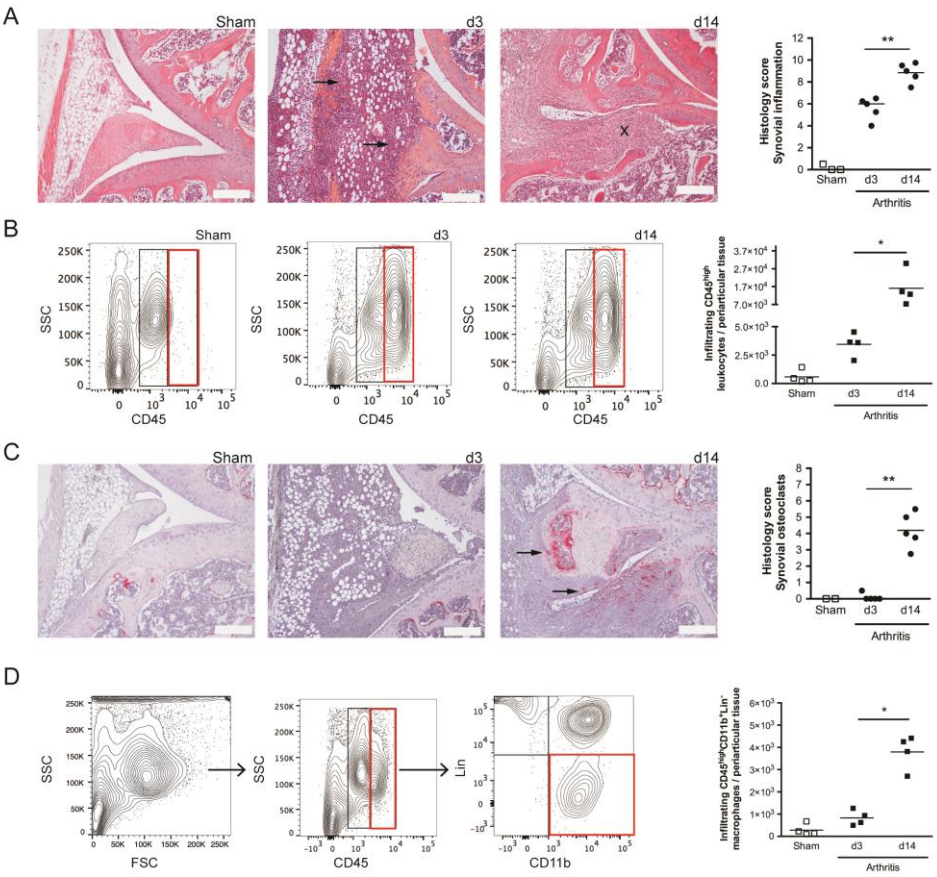

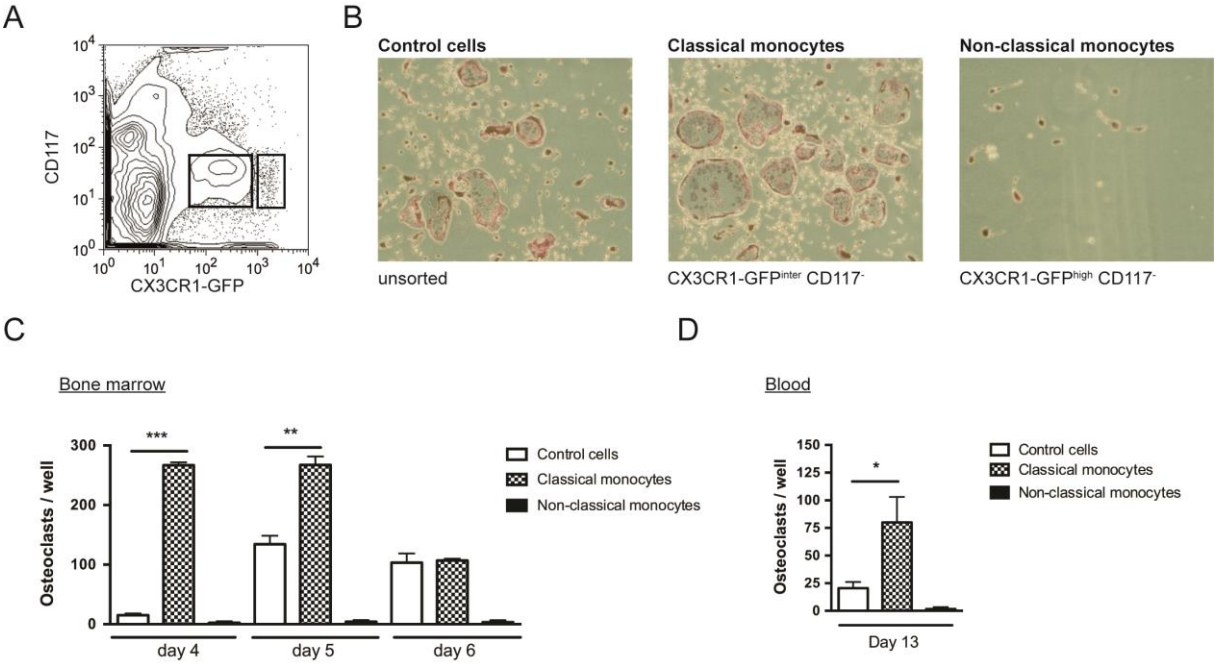

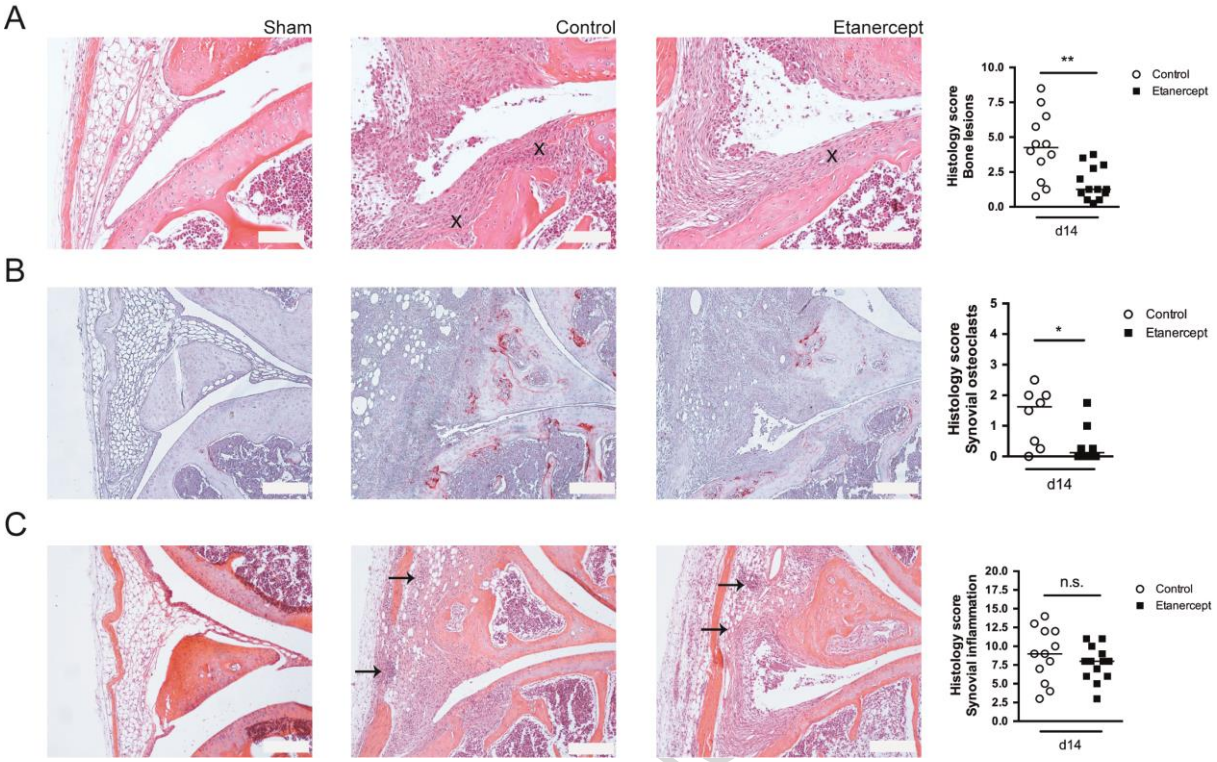

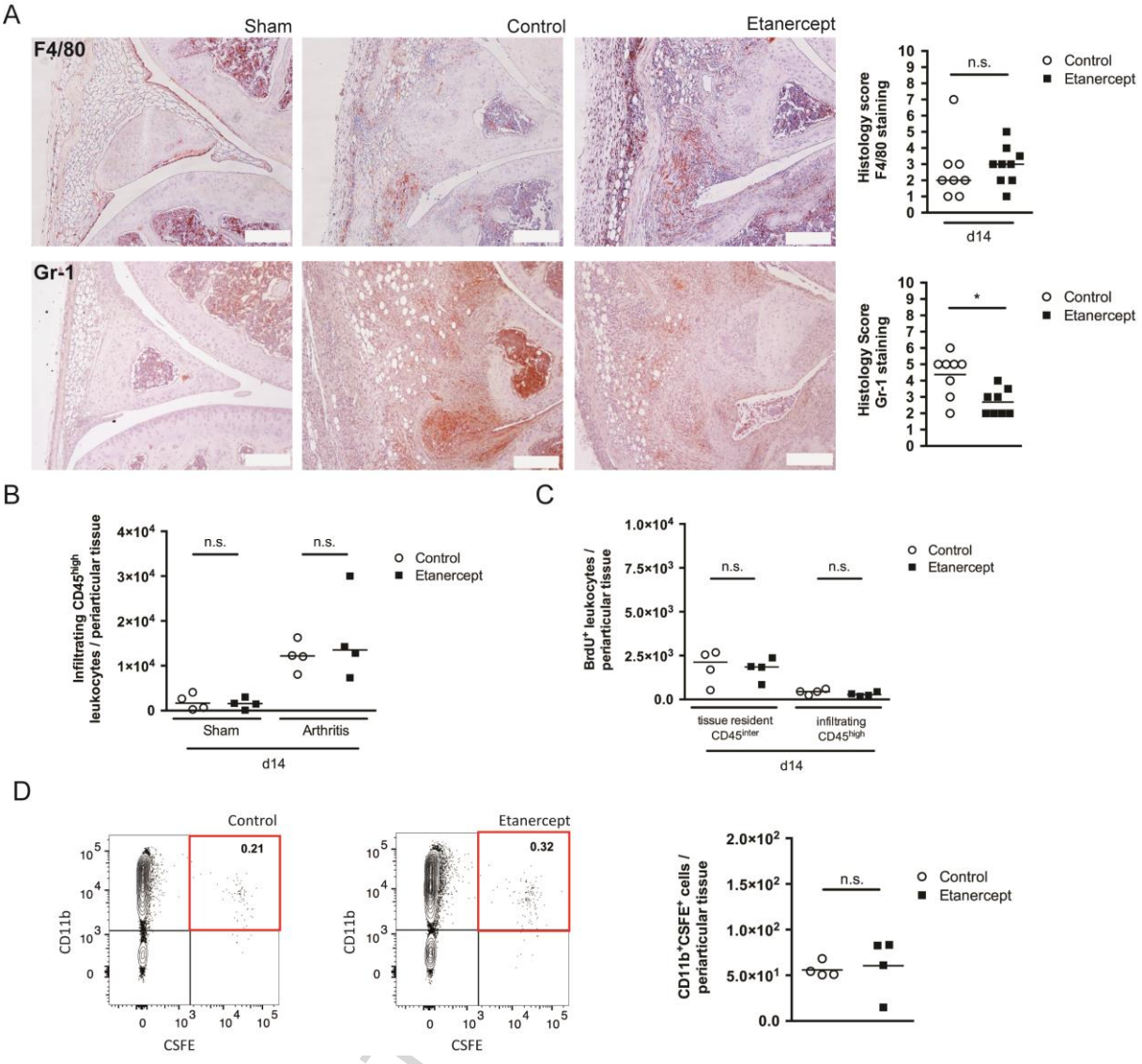

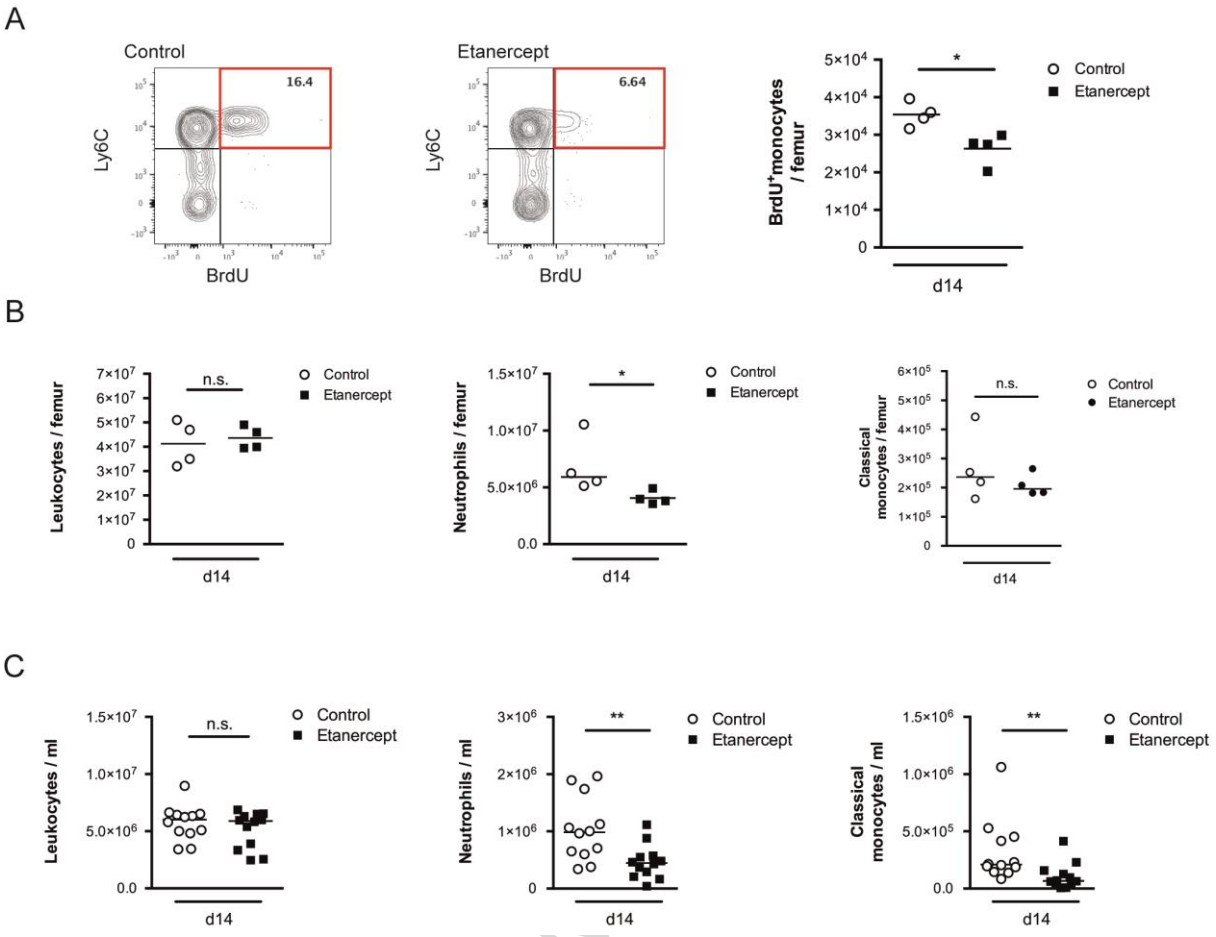

Highlights

TNFα blockade mediates bone protection in antigen - induced arthritis by reducing osteoclast precursor supply

Synovial bone lesions and osteoclasts are markedly reduced upon etanercept in the early chronic phase of AIA, which is not associated with a reduced recruitment of circulating OPCs to the arthritic joint nor to reduced synovial inflammation.

OPC numbers in bone marrow and blood are significantly reduced upon etanercept treatment.

Arrest of osteoclast mediated bone lesions in AIA upon inhibition of TNFα is based on reduced OPC availability in the periphery, and not on OPC recruitment or local anti-inflammatory effects in the arthritic joint.